

Yoshitake Sakae^a and Yuko Okamoto^{a,b}

^a*Department of Functional Molecular Science
The Graduate University for Advanced Studies
Okazaki, Aichi 444-8585, Japan*

and

^b*Department of Theoretical Studies
Institute for Molecular Science
Okazaki, Aichi 444-8585, Japan*

Abstract

We propose a novel method to optimize existing force-field parameters for protein systems. The method consists of minimizing the summation of the square of the force acting on each atom in the proteins with the structures from the Protein Data Bank. We performed this optimization to the partial-charge and torsion-energy parameters of the AMBER parm96 force field, using 100 molecules from the Protein Data Bank. We then performed folding simulations of α -helical and β -hairpin peptides. The optimized force-field parameters gave structures more similar to the experimental implications than the original AMBER force field.

1 Introduction

In the theoretical studies of biomolecular systems, it is now indispensable to use molecular simulation techniques such as Monte Carlo (MC) and molecular dynamics (MD) methods. Most such simulations use the potential energy functions within the framework of classical mechanics consisting of certain energy terms with force-field parameters. Well-known force fields (or potential energy functions) are AMBER [1]–[3], CHARMM [4], OPLS [5, 6], GROMOS [7], and ECEPP [8]. These force fields have been parameterized to fit experimental data of small molecules and, for some terms, quantum chemistry calculations. In fact, it is rather difficult to test the validity of these force-field parameters, because simulations of biomolecular systems will be hampered by the multiple-minima problem; the simulations will get trapped in states of energy local minima and will yield unreliable results. Hence, it is essential to employ powerful simulation algorithms such as generalized-ensemble algorithms (for a recent review, see Ref. [9]) in order to have accurate comparisons of force fields. For instance, we have recently carried out detailed comparisons of three versions (parm94 [1], parm96 [2], and parm99 [3]) of AMBER, CHARMM [4], OPLS-AA/L [6], and GROMOS [7] by generalized-ensemble simulations of small peptides [10].

If any problems are found in the force fields, we have to improve the force-field parameters by some means. In this Letter, we propose a novel method for optimization of force-field parameters. Our method utilizes the protein structures in the Protein Data Bank (PDB) [24], in which the number of entries is rapidly increasing. Actually, there already exist many works of similar knowledge-based methods of force-field development [11]–[22]. Our method is different from most of previous works in two points: we deal with all-atom force fields such as AMBER, and we use only the PDB data without introducing so-called decoys (or, misfolded structures).

In section 2 the details of the formulation of our method are described. In section 3 an example of the application of our method is presented. Conclusions and future prospects are presented in section 4.

2 Methods

The existing all-atom force fields for protein systems such as AMBER and CHARMM use essentially the same functional forms for the conformational potential energy E_{conf} except for minor differences. E_{conf} can be written as, for instance,

$$E_{\text{conf}} = E_{\text{BL}} + E_{\text{BA}} + E_{\text{torsion}} + E_{\text{nonbond}} , \quad (1)$$

$$E_{\text{BL}} = \sum_{\text{bond length } \ell} K_{\ell}(\ell - \ell_{\text{eq}})^2 , \quad (2)$$

$$E_{\text{BA}} = \sum_{\text{bond angle } \theta} K_{\theta}(\theta - \theta_{\text{eq}})^2 , \quad (3)$$

$$E_{\text{torsion}} = \sum_{\text{dihedral angle } \Phi} \sum_n \frac{V_n}{2} [1 + \cos(n\Phi - \gamma_n)] , \quad (4)$$

$$E_{\text{nonbond}} = \sum_{i < j} \left[\frac{A_{ij}}{r_{ij}^{12}} - \frac{B_{ij}}{r_{ij}^6} + \frac{q_i q_j}{\epsilon r_{ij}} \right] . \quad (5)$$

Here, E_{BL} , E_{BA} , and E_{torsion} represent the bond-stretching term, the bond-bending term, and the torsion-energy term, respectively. The bond-stretching and bond-bending energies are given by harmonic terms with the force constants K_{ℓ} and K_{θ} , and the equilibrium positions, ℓ_{eq} and θ_{eq} . The torsion energy is, on the other hand, described by the Fourier series in Eq. (4), where the sum is taken over all dihedral angles Φ , n is the number of waves, γ_n is the phase, and V_n is the Fourier coefficient. The nonbonded energy in Eq. (5) is represented by the Lennard-Jones and Coulomb terms between pairs of atoms, i and j , separated by the distance r_{ij} . The parameters A_{ij} and B_{ij} in Eq. (5) are the coefficients for the Lennard-Jones term, q_i is the partial charge of the i -th atom in the electrostatic term, and ϵ is the dielectric constant, where we set $\epsilon = 1$. Hence, we have five classes of force-field parameters, namely, those in the bond-stretching term (K_{ℓ} and ℓ_{eq}), those in the bond-bending term (K_{θ} and θ_{eq}), those in the torsion term (V_n and γ_n), those in the Lennard-Jones term (A_{ij} and B_{ij}), and those in the electrostatic term (q_i).

We now describe our new method for optimizing these force-field parameters. We first select N molecules in PDB. We try to choose proteins from different folds (such as all α -helix, all β -sheet, α/β , etc.) and different homology classes as much as possible. If the

force-field parameters are of ideal values, we expect that all the chosen native structures are stable without any force acting on each atom in the molecules. Hence, we expect

$$F = 0 , \quad (6)$$

where

$$F = \sum_{m=1}^N \frac{1}{N_m} \sum_{i_m=1}^{N_m} |\vec{f}_{i_m}|^2 , \quad (7)$$

and

$$\vec{f}_{i_m} = -\frac{\partial E_{\text{tot}}}{\partial \vec{x}_{i_m}} . \quad (8)$$

Here, N_m is the total number of atoms in molecule m , E_{tot} is the total potential energy, and \vec{f}_i is the force acting on atom i . In reality, $F \neq 0$, and because $F \geq 0$, we expect that we can optimize the force-field parameters by minimizing F with respect to these parameters. In practice, we perform a simulation in the force-field parameter space for this minimization.

Proteins are usually in aqueous solution, and hence we also have to incorporate some kind of solvent effects. Because the more the total number of proteins (N) is, the better the force-field parameter optimizations are expected to be, we want to minimize our efforts in the calculations of the solvent effects. Here, we employ the generalized-Born/surface area (GB/SA) terms for the solvent contributions [25, 26]. Hence, we use in Eq. (8)

$$E_{\text{tot}} = E_{\text{conf}} + E_{\text{solv}} , \quad (9)$$

where

$$E_{\text{solv}} = E_{\text{GB}} + E_{\text{SA}} , \quad (10)$$

$$E_{\text{GB}} = -166 \left(1 - \frac{1}{\epsilon_s}\right) \sum_{i,j} \frac{q_i q_j}{\sqrt{r_{ij}^2 + \alpha_{ij}^2} e^{-D_{ij}}} , \quad (11)$$

$$E_{\text{SA}} = \sum_k \sigma_k A_k . \quad (12)$$

Namely, in the GB/SA model, the total solvation free energy in Eq. (10) is given by the sum of a solute-solvent electrostatic polarization term, a solvent-solvent cavity term, and a solute-solvent van der Waals term. A solute-solvent electrostatic polarization term can be calculated by the generalized Born equation (11), where $\alpha_{ij} = \sqrt{\alpha_i \alpha_j}$, α_i is the so-called Born radius of atom i , $D_{ij} = r_{ij}^2 / (2\alpha_{ij})^2$, and ϵ_s is the dielectric constant of bulk water (we take $\epsilon_s = 78.3$). A solvent-solvent cavity term and a solute-solvent van der Waals term can be approximated by the term that is proportional to the solvent accessible surface area in Eq. (12). Here, A_k is the total solvent-accessible surface area of atoms of type k and σ_k is an empirically determined proportionality constant [25, 26].

The flowchart of our method for the optimization of force-field parameters is shown in Fig. 1.

In Step 1 we try to obtain as many structures as possible from PDB. The number is limited by the computer power that we have available in our laboratory. We want to choose proteins with different sizes (numbers of amino acids), different folds, and different homology classes as much as possible. We also want to use only those with high experimental resolutions. Note that only atomic coordinates of proteins are extracted from PDB (and coordinates from other molecules such as crystal water are neglected).

If we use data from X-ray experiments, hydrogen atoms are missing, and thus in Step 2 we have to add hydrogen coordinates. Many protein simulation software packages provide with routines that add hydrogen atoms to the PDB coordinates, and one can use one of such routines.

We now have N protein coordinates ready, but usually such “raw data” result in very high total potential energy and strong forces will be acting on some of the atoms in the molecules. This is because the hydrogen coordinates we added as above are not based on experimental results and have rather large uncertainties. The coordinates of heavy atoms from PDB also have experimental uncertainties. We take the position that we leave the coordinates of heavy atoms as they are in PDB as much as possible, and adjust the hydrogen coordinates to adjust this mismatch. This is why we want to include as many PDB data as possible with high experimental resolution (so that the effects of experimental errors in PDB may be minimal). We thus minimize the total potential energy $E_{\text{tot}} = E_{\text{conf}} + E_{\text{solv}} + E_{\text{constr}}$ with respect to the coordinates for each protein conformation, where E_{constr} is the constraint energy term that is imposed on the heavy atoms in PDB (it is referred to as the “predefined constraints” in Steps 3 and 5 in Fig. 1):

$$E_{\text{constr}} = \sum_{\text{heavy atom}} K_x (\vec{x} - \vec{x}_0)^2 . \quad (13)$$

Here, K_x is the force constants of the restriction (in the present work, we use the value of 100 kcal/mol/Å²), and \vec{x}_0 are the original coordinate vectors of heavy atoms in PDB. Because we are searching for the nearest local-minimum states, usual minimization routines such as conjugate-gradient method and Newton-Raphson method can be employed here. As one can see from Eq. (13), the coordinates of hydrogen atoms will be mainly adjusted, but unnatural heavy-atom coordinates will also be modified. We perform this minimization for all N protein structures separately, and obtain N refined structures.

Given N set of “ideal” reference coordinates in Step 3, we now optimize the first set of force-field parameters in Step 4. In Eq. (1) we have five classes of force-field parameters as mentioned above. Namely, the force-field parameters are those in the bond-stretching term (K_ℓ and ℓ_{eq}), those in the bond-bending term (K_θ and θ_{eq}), those in the torsion term (V_n and γ_n), those in the Lennard-Jones term (A_{ij} and B_{ij}), and those in the electrostatic term (q_i). Because they are of very different nature, we believe that it is better to optimize these classes of force-field parameters separately (as in Steps 4, 6, and so on in Fig. 1). For each set of force-field parameters, the optimization is carried out by minimizing F in Eq. (7) with respect to these parameters. Here, E_{tot} in Eq. (8) is given by Eq. (9) For this purpose usual minimization routines such as conjugate-gradient method are not adequate, because we need a global optimization. One can employ more powerful methods such as simulated annealing [23] and generalized-ensemble algorithms [9]. We perform this minimization simulation in the above parameter space to obtain the parameter values that give the global minimum of F .

These processes are repeated until the optimized force-field parameters converge.

We can, in principle, optimize all the force-field parameters following the flowchart in Fig. 1. In the example given in the next section, however, we just optimize two classes of the force-field parameters; namely, the partial charges (q_i) and the backbone torsion energy parameters (V_1 , V_2 , and V_3). Here, we fix the phases (γ_n) and the main-chain

torsion energy term is written as (see Eq. (4))

$$E_{\Phi=\phi,\psi} = \frac{V_1}{2} [1 + \cos(\Phi)] + \frac{V_2}{2} [1 + \cos(2\Phi - \pi)] + \frac{V_3}{2} [1 + \cos(3\Phi)] \quad , \quad (14)$$

for each backbone dihedral angle ϕ and ψ . As for the partial charge optimization, we impose a condition that the total charge of each amino acid remains constant, which is the usual assumption adopted by force fields of Eqs. (2)–(5) based on classical mechanics.

We believe that these two classes of parameters have the most uncertainty among all the force-field parameters. This is because partial charges are usually obtained by quantum chemistry calculations of an isolated amino acid in vacuum separately, which is a very different condition from that in amino acids of proteins in aqueous solution and because torsion-energy term is the most problematic (for instance, parm94, parm96, and parm99 versions of AMBER differ mainly in torsion-energy parameters).

3 Results and discussion

We now present an example of the application of our force-field optimization scheme presented in the previous section. The force field that we optimized is the AMBER parm96 version [2]. We have optimized two sets of parameters. The first set is the partial charge parameters (q_i in Eq. (5)) and there are 602 such parameters altogether in AMBER. The second set is the backbone torsion-energy parameters (V_1 , V_2 , and V_3 in Eq. (14)) and there are six such parameters (three each for ϕ and ψ). We used the program package TINKER [27] for all the calculations in the present work.

In Step 1 of the flowchart of Fig. 1, we chose 100 PDB files ($N = 100$) with resolution 1.8 Å or better and with less than 200 residues (the average number of residues is 120.4) from PISCES [28]. Their PDB code names are 2LIS, 1EP0, 1TIF, 1EB6, 1C1L, 1CCW, 2PTH, 1I6W, 1DBF, 1KPF, 1LRI, 1AAP, 1C75, 1CC8, 1FK5, 1KQR, 1K1E, 1CZP, 1GP0, 1KOI, 1IQZ, 3EBX, 1I40, 1EJG, 1AMM, 1I07, 1GK8, 1GVP, 1M4I, 1EYV, 1E29, 1I2T, 1VCC, 1FM0, 1EXR, 1GUT, 1H4X, 1GBS, 1B0B, 1I9L, 1IFC, 1DLW, 1EAJ, 1GGZ, 1JR8, 1RB9, 1VAP, 1JZG, 1M55, 1EN2, 1C9O, 2ERL, 1EMV, 1F41, 1EW6, 2TNF, 1IFR, 1JSE, 1KAF, 1HZT, 1HQK, 1FXL, 1BKR, 1ID0, 1LQV, 1G2R, 1KR7, 1QTN, 1D4O, 1EAZ, 2CY3, 1UGI, 1IJV, 3VUB, 1BZP, 1JYR, 1DZK, 1QFT, 1UTG, 2CPG, 1I6W, 1C7K, 1I8O, 1LO7, 1LNI, 1EQO, 1NDD, 1HD2, 3PYP, 1FD3, 1DK8, 1WHI, 1FAZ, 4FGF, 2MHR, 1JB3, 2MCM, 1IGD, 1C5E, and 1JIG.

The minimization for the coordinate refinement in Step 3 of the flowchart was done with the constraint of Eq. (13). In Fig. 2(a), a part of the original PDB structure of one of the molecules (2LIS) and the corresponding part in the refined structure are superposed. As expected, we see good coincidence of heavy-atom coordinates and small deviations in the hydrogen coordinates. RMSD (Root Mean Square Distance) (for heavy atoms) of these two conformations of the entire molecule (2LIS) is indeed small: 0.027 Å (the average of all 100 proteins is 0.03 Å).

As also expected, the structure of the raw PDB data (that obtained in Step 2 of the flowchart) is not stable in the sense that the force acting on some atoms in the molecule will be large, while the refined structure (that obtained in Step 3 of the flowchart) will not have abnormally large forces acting. This is illustrated in Fig. 2(b). The average absolute value of the components of the force before minimization and after minimization is 9.0 kcal/mol/Å and 1.5 kcal/mol/Å, respectively.

In Step 4 of the flowchart, we performed the optimization of partial-charge parameters by MC simulated annealing. Namely, we minimized F in Eq. (7) by MC simulated annealing simulations of these parameters (the parameters are updated and the updates are accepted or rejected according to the Metropolis criterion). For this we introduced an effective “temperature” for the parameter space. Each simulation run consisted of 50,000 MC sweeps with the temperature decreased exponentially from 200 to 0.01. The simulation was repeated 10 times with different initial random numbers. The time series of F from one of the simulations is shown in Fig. 3(a). We see that F decreases quickly in the beginning until about 5,000 MC sweeps and then it decreases very slowly; the total number of MC sweeps (50,000) seems sufficient. The optimized partial charges are taken from those that resulted in the lowest F value.

Each term contributing to F (i.e., each component of the force acting on the atoms) before and after the optimization is compared in Fig. 2(c). We see that many terms decreased in magnitude as a whole.

In Tables 1, 2, and 3, three examples (alanine, glutamic acid, and tyrosine) of the obtained partial charges together with the original AMBER values are listed. The magnitudes of the charges seem to decrease a little in general, although there are exceptions (see, for instance, CG and CE of tyrosine). Although the sign of the partial charges remains the same for those with large magnitude, charges with small magnitude sometimes change their sign (see, for example, CG of glutamic acid and CA, CB, and HB of tyrosine).

In Step 5 of the flowchart, the original coordinates obtained in Step 2 were again minimized with the constraint of Eq. (13), but this time the optimized parameters were used. The average RMSD of 100 proteins is 0.03 Å, and the coordinates of heavy atoms have little changed.

In Step 6 of the flowchart, we carried out the optimization of the six torsion-energy parameters (V_1 , V_2 , and V_3 in Eq. (14) for both ϕ and ψ) by minimizing F in Eq. (7) with MC simulated annealing simulations in this parameter space. Each simulation run consisted of 10,000 MC sweeps with the temperature decreasing from 1,000 to 1.0. The simulation was repeated several times with different random numbers, but the six optimized parameters all agreed with one another. The time series of F from one of the simulations is shown in Fig. 3(b), and the obtained torsion-energy parameters are listed in Table 4. Each term contributing to F before and after the optimization is compared in Fig. 2(d). The term corresponding to the backbone atoms that are relevant to the torsion-energy parameters decreased, as expected. Non-zero contributions are presumably to be reduced by optimization of other force-field parameters.

In the present example, we stopped our process in Step 6 of the flowchart and did not iterate the optimizations.

We tested the effectiveness of the new force field by applying it to the folding simulations of two peptides, C-peptide of ribonuclease A and the C-terminal fragment of the B1 domain of streptococcal protein G, which is sometimes referred to as G-peptide [31]. The C-peptide has 13 residues and its amino-acid sequence is Lys-Glu-Thr-Ala-Ala-Lys-Phe-Glu-Arg-Gln-His-Met. This peptide has been extensively studied by experiments and is known to form an α -helix structure [29, 30]. Because the charges at peptide termini are known to affect helix stability [29, 30], we blocked the termini by a neutral COCH₃- group and a neutral -NH₂ group. The G-peptide has 16 residues and its amino-acid sequence is Gly-Glu-Trp-Thr-Tyr-Asp-Asp-Ala-Thr-Lys-Thr-Phe-Thr-Val-Thr-Glu. The termini were kept as the usual zwitter ionic states, following the experimental con-

ditions [32, 33, 31]. This peptide is known to form a β -hairpin structure by experiments [32, 33, 31].

Simulated annealing MD simulations of 1 ns were performed for both peptides from extended initial conformations. The unit time step was set to 1.0 fs (hence, each run consists of 1,000,000 MD steps). The temperature during MD simulations was controlled by Berendsen’s method [34]. For each simulation the temperature was decreased from 2,000 K to 200 K. As for solvent effects, in order to carry out quantitative test, we want to include accurate contributions such as explicit water molecules. Here, for simplicity, however, we used the GB/SA model in Eqs. (10)–(12) was used. For both peptides, these folding simulations were repeated 16 times with different initial conformations. As for force fields, both the original AMBER parm96 force field and the optimized force field were used.

In Fig. 4 the lowest-energy conformations of C-peptide obtained from each of the folding simulations are shown. They are numbered in increasing order of energy. Almost all conformations are α -helix structure in the case of the original AMBER parm96 (see Fig. 4(a)), although a short β -hairpin structure is also found in two conformations (Nos. 12 and 16). RMSD (only C_α atoms are taken into account) from the corresponding part of the native X-ray structure of the entire ribonulcease A was the lowest for conformations Nos. 3 (2.47 Å), 14 (2.59 Å), and 15 (2.81 Å). For the optimized force field (see Fig. 4(b)), five out of 16 conformations (Nos. 2, 7, 8, 9, and 11) are α -helix structure, and β -hairpin structure also appeared in Nos. 12, 14, and 15. Though both α -helix and β -hairpin structures appear with the optimized force field, α -helix is more favored than β -hairpin in the sense that the energy is lower for conformations with α -helix than those with β -hairpin. RMSD was the lowest for conformations Nos. 13 (3.17 Å), 16 (3.50 Å), and 11 (3.51 Å). Although the original AMBER parm96 gave more conformations closer to the native structure (smaller RMSD) than the optimized force field, it seems to favor α -helix too much. The experiments imply only 30 % α -helix formations around 0° C [29], which is more consistent with the results for the optimized force field.

In Fig. 5 the lowest-energy conformations of G-peptide obtained from the folding simulations are shown. The results for the original AMBER parm96 (see Fig. 5(a)), are again almost all α -helical. This is in contradiction with the experimental results [32, 33, 31] which imply the formation of a β -hairpin. RMSD from the corresponding part of the native X-ray structure of the entire protein G was the lowest for conformations Nos. 14 (4.52 Å), 13 (5.30 Å), and 8 (5.53 Å). For the optimized force field (see Fig. 5(b)), as many as eight out of 16 conformations (Nos. 3, 4, 5, 8, 10, 11, 14, and 15) yielded β -hairpin structure, and α -helix structure also appeared in Nos. 5 and 14. RMSD was the lowest for conformations Nos. 7 (3.74 Å), 4 (3.84 Å), and 11 (4.00 Å). Hence, for the case of G-peptide, the improvement of the force field by our optimization procedure is great (both in secondary structure content and in RMSD).

4 Conclusions

In this Letter, we proposed a novel method to optimize the force-field parameters for protein systems. Our method is knowledge-based in the sense that we utilize the protein structures in the Protein Data Bank. With this method one can optimize not only the existing force-field parameters such as AMBER, CHARMM, OPLS, and so on, but also

any force field as long as its functional form is given.

We have presented an example of the application of the present method to the original AMBER parm96 force field by optimizing the partial-charge and backbone torsion-energy parameters. There is still a lot of testing to be done. For instance, other parameter sets in AMBER parm96 as well as other force fields should also be tried. We used only 100 protein structures, and this number should be increased. As for solvent effects in the optimization procedure, we employed the generalized-Born/surface area model, but the validity of this approximation should be tested. Namely, we have to check how insensitive or sensitive the final optimized parameters are to the solvation theory used. Finally, because the parameter space we optimize may be large, we want to use a more powerful optimization algorithm than simulated annealing. Generalized-ensemble algorithm [9] may be one choice of such optimization methods.

Acknowledgements:

The computations were performed on the computers at the Research Center for Computational Science, Okazaki National Research Institutes and at ITBL, Japan Atomic Energy Research Institute. This work was supported, in part, by the NAREGI Nanoscience Project, Ministry of Education, Culture, Sports, Science and Technology, Japan.

References

- [1] W.D. Cornell, P. Cieplak, C.I. Bayly, I.R. Gould, K.M. Merz Jr., D.M. Ferguson, D.C. Spellmeyer, T. Fox, J.W. Caldwell, P.A. Kollman, *J. Am. Chem. Soc.* 117 (1995) 5179.
- [2] P.A. Kollman, R. Dixon, W. Cornell, T. Fox, C. Chipot, A. Pohorille, *Computer Simulation of Biomolecular Systems*, Eds. A. Wilkinson, P. Weiner and W.F. van Gunsteren 3 (1997) 83.
- [3] J. Wang, P. Cieplak, P.A. Kollman, *J. Comput. Chem.* 21 (2000) 1049
- [4] A.D. MacKerrell, Jr., D. Bashford, M. Bellott, R.L. Dunbrack, Jr., J.D. Evanseck, M.J. Field, S. Fischer, J. Gao, H. Guo, S. Ha, D. Joseph-McCarthy, L. Kuchnir, K. Kuczera, F.T.K. Lau, C. Mattos, S. Michnick, T. Ngo, D.T. Nguyen, B. Prodhom, W.E. Reiher, III, B. Roux, M. Schlenkrich, J.C. Smith, R. Stote, J. Straub, M. Watanabe, J. Wiórkiewicz-Kuczera, D. Yin, M. Karplus, *J. Phys. Chem. B* 102 (1998) 3586.
- [5] W.L. Jorgensen, D.S. Maxwell, J. Tirado-Rives, *J. Am. Chem. Soc.* 118 (1996) 11225.
- [6] G.A. Kaminski, R.A. Friesner, J. Tirado-Rives, W.L. Jorgensen, *J. Phys. Chem. B* 105 (2001) 6474.
- [7] W.F. van Gunsteren, S.R. Billeter, A.A. Eising, P.H. Hünenberger, P. Krüger, A.E. Mark, W.R.P. Scott, I.G. Tironi (1996) *Biomolecular simulation: the GROMOS96 manual and user guide*. Zürich: Vdf Hochschulverlag AG an der ETH Zürich.
- [8] M.J. Sippl, G. Némethy, H.A. Scheraga, *J. Phys. Chem.* 88 (1984) 6231, and references therein.

- [9] A. Mitsutake, Y. Sugita, Y. Okamoto, *Biopolymers (Pept. Sci.)* 60 (2001) 96.
- [10] T. Yoda, Y. Sugita, Y. Okamoto, in preparation.
- [11] S. Tanaka, H.A. Scheraga, *Macromol.* 9 (1976) 945.
- [12] S. Miyazawa, R.L. Jernigan, *Macromol.* 18 (1985) 534.
- [13] M.J. Sippl, *J. Mol. Biol.* 213 (1990) 859.
- [14] R.A. Goldstein, Z.A. Luthey-Schulten, P.G. Wolynes, *Proc. Natl. Acad. Sci. U.S.A.* 89 (1992) 4918.
- [15] V.N. Maiorov, G.M. Crippen, *J. Mol. Biol.* 227 (1992) 876.
- [16] K. Nishikawa, Y. Matsuo, *Protein Eng.* 6 (1993) 811.
- [17] A. Godzik, A. Kolinski, J. Skolnick, *Protein Sci.* 4 (1995) 2107.
- [18] L.A. Mirny, E.I. Shakhnovich, *J. Mol. Biol.* 264 (1996) 1164.
- [19] K.T. Simons, C. Kooperberg, E. Huang, D. Baker, *J. Mol. Biol.* 268 (1997) 209.
- [20] R. Samudrala, J. Moult, *J. Mol. Biol.* 275 (1998) 895.
- [21] S. Takada, Z.A. Luthey-Schulten, P.G. Wolynes, *J. Chem. Phys.* 110 (1999) 11616.
- [22] Y. Xia, M. Levitt, *J. Chem. Phys.* 113 (2000) 9318.
- [23] S. Kirkpatrick, C.D. Gelatt Jr., M.P. Vecchi, *Science* 220 (1983) 671.
- [24] H.M. Berman, J. Westbrook, Z. Feng, G. Gilliland, T.N. Bhat, H. Weissig, I.N. Shindyalov, P.E. Bourne, *Nucleic Acids Research* 28 (2000) 235.
- [25] W.C. Still, A. Tempczyk, R.C. Hawley, T. Hendrickson, *J. Am. Chem. Soc.* 112 (1990) 6127.
- [26] D. Qiu, P.S. Shenkin, F.P. Hollinger, W.C. Still, *J. Phys. Chem. A* 101 (1997) 3005.
- [27] <http://dasher.wustl.edu/tinker/>.
- [28] <http://www.fccc.edu/research/labs/dunbrack/pisces/>.
- [29] K.R. Shoemaker, P.S. Kim, D.N. Brems, S. Marqusee, E.J. York, I.M. Chaiken, J.M. Stewart, R.L. Baldwin, *Proc. Natl. Acad. Sci. U.S.A.* 82 (1985) 2349.
- [30] J.J. Osterhout Jr., R.L. Baldwin, E.J. York, J.M. Stewart, H.J. Dyson, P.E. Wright, *Biochemistry* 28 (1989) 7059.
- [31] S. Honda, N. Kobayashi, E. Munekata, *J. Mol. Biol.* 295 (2000) 269.
- [32] F.J. Blanco, G. Rivas, L. Serrano, *Nature Struct. Biol.* 1 (1994) 584.
- [33] N. Kobayashi, S. Honda, H. Yoshii, H. Uedaira, E. Munekata, *FEBS Lett.* 366 (1995) 99.

- [34] H.J.C. Berendsen, J.P.M. Postma, W.F. van Gunsteren, A. DiNola, J.R. Haak, J. Chem. Phys. 81 (1984) 3684.
- [35] R.A. Sayle, E.J. Milner-White, Trends Biochem. Sci. 20 (1995) 374.

Table 1: Partial-charge parameters of alanine

Atom	parm96	optimized
N	-0.4157	-0.3317
CA	0.0337	0.0628
C	0.5973	0.4996
HN	0.2719	0.2358
O	-0.5679	-0.5533
HA	0.0823	0.0923
CB	-0.1825	-0.0394
HB	0.0603	0.0112
Total	0.0000	-0.0003

Table 2: Partial-charge parameters of glutamic acid

Atom	parm96	optimized
N	-0.5163	-0.4207
CA	0.0397	0.0642
C	0.5366	0.4635
HN	0.2936	0.2618
O	-0.5819	-0.6054
HA	0.1105	0.1255
CB	0.0560	0.1215
HB	-0.0173	-0.0387
CG	0.0136	-0.0724
HG	-0.0425	-0.0307
CD	0.8054	0.8307
OE	-0.8188	-0.8149
Total	-1.0000	-0.9999

Table 3: Partial-charge parameters of tyrosine

Atom	parm96	optimized
N	-0.4157	-0.3492
CA	-0.0014	0.0437
C	0.5973	0.5467
HN	0.2719	0.2480
O	-0.5679	-0.5705
HA	0.0876	0.0969
CB	-0.0152	0.0673
HB	0.0295	-0.0098
CG	-0.0011	-0.2136
CD	-0.1906	0.0974
HD	0.1699	0.0636
CE	-0.2341	-0.3145
HE	0.1656	0.1376
CZ	0.3226	0.2875
OH	-0.5579	-0.5024
HH	0.3992	0.3968
Total	0.0000	-0.0002

Table 4: Backbone torsion-energy parameters

Dihedral angle	$V_1/2$	$V_2/2$	$V_3/2$
ϕ (parm96)	0.850	0.300	0.0
ϕ (optimized)	1.209	0.380	-0.018
ψ (parm96)	0.850	0.300	0.0
ψ (optimized)	0.133	0.578	0.050

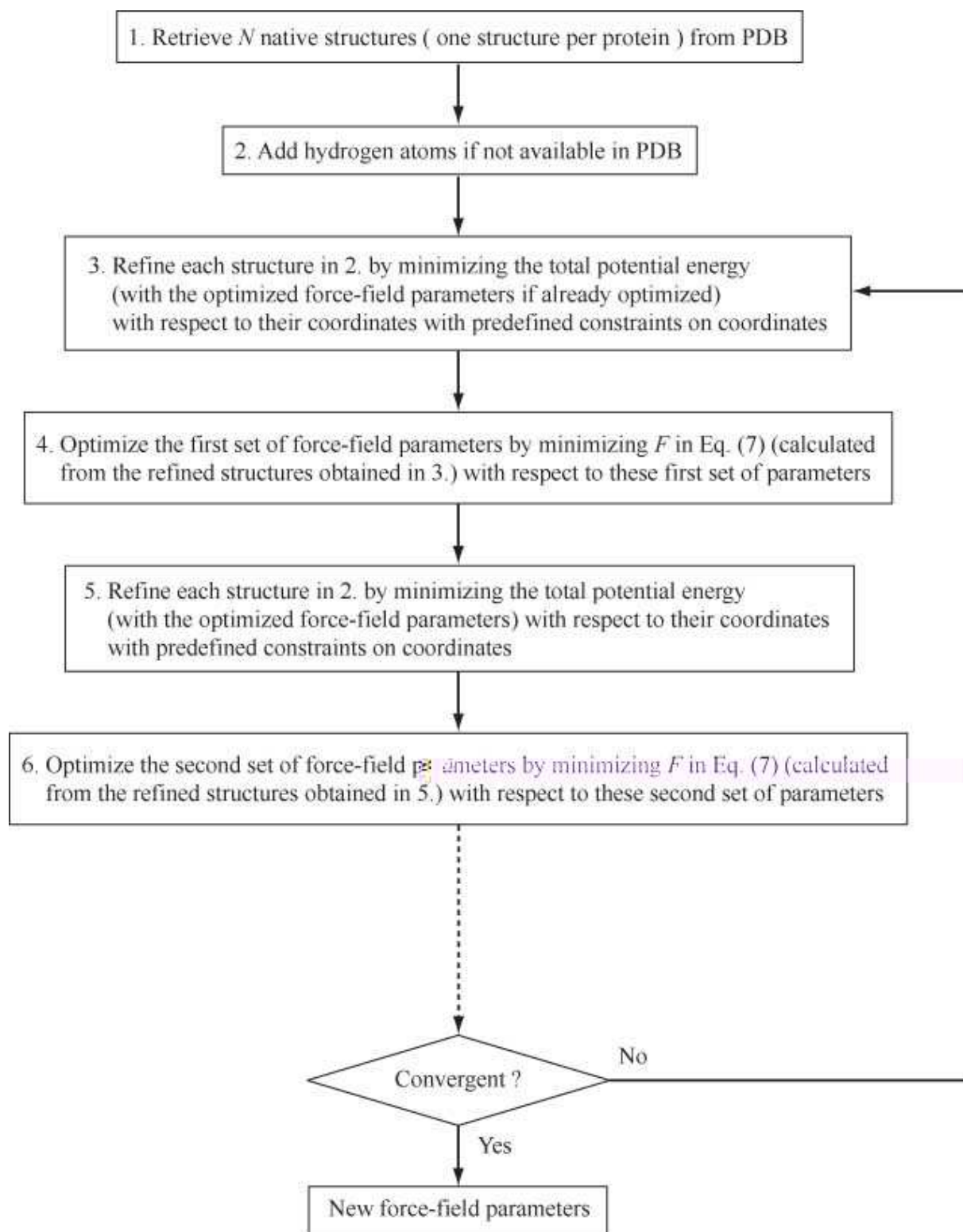


Figure 1: The flowchart of our method for the optimization of force-field parameters.

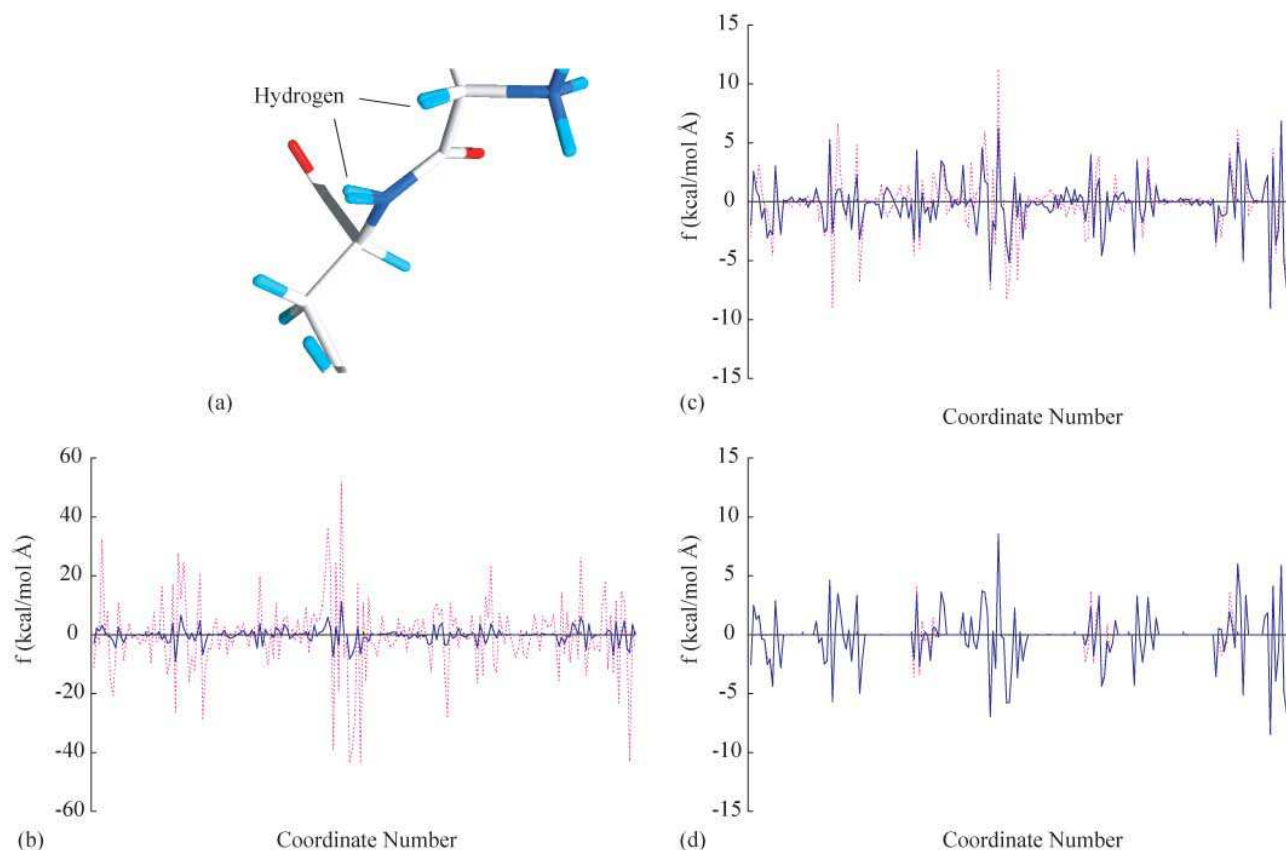


Figure 2: (a) Superposition of a part of the original PDB structure (PDB code: 2LIS) with hydrogen atoms added and the corresponding part in the refined structure. These structures were obtained in Steps 2 and 3 of the flowchart in Fig. 1. (b) Components of the force acting on the atoms in the original structure of 2LIS (red dotted curve) and its refined structure (blue solid curve). The structures are the same as those in (a). The force field is the original AMBER parm96. (c) Components of the force acting on the atoms in the refined structure of 2LIS. The force field is the original AMBER parm96 (red dotted curve) and AMBER parm96 with the partial-charge parameters optimized (blue solid curve). (d) Components of the force acting on the atoms in the refined structure of 2LIS. The force field is the original AMBER parm96 with the partial-charge parameters optimized (red dotted curve) and AMBER parm96 with the partial-charge and torsion-energy parameters optimized (blue solid curve). In (b), (c), and (d), only 200 components are shown.

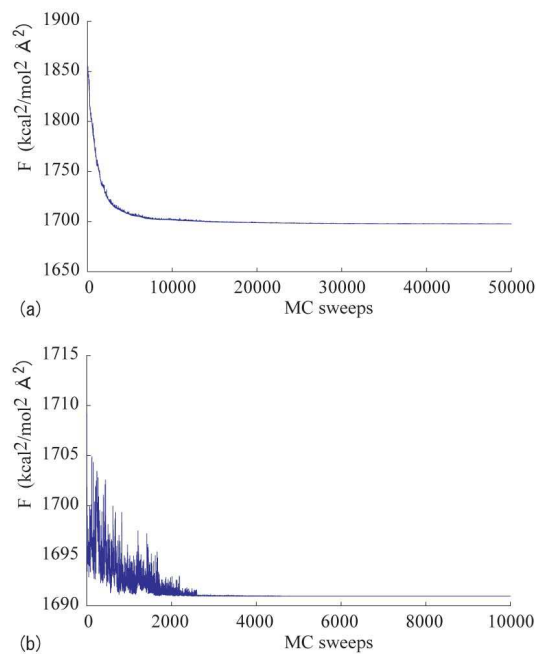


Figure 3: Time series of MC simulated annealing simulations in force-field parameter space for partial-charge (a) and torsion-energy (b) parameters.

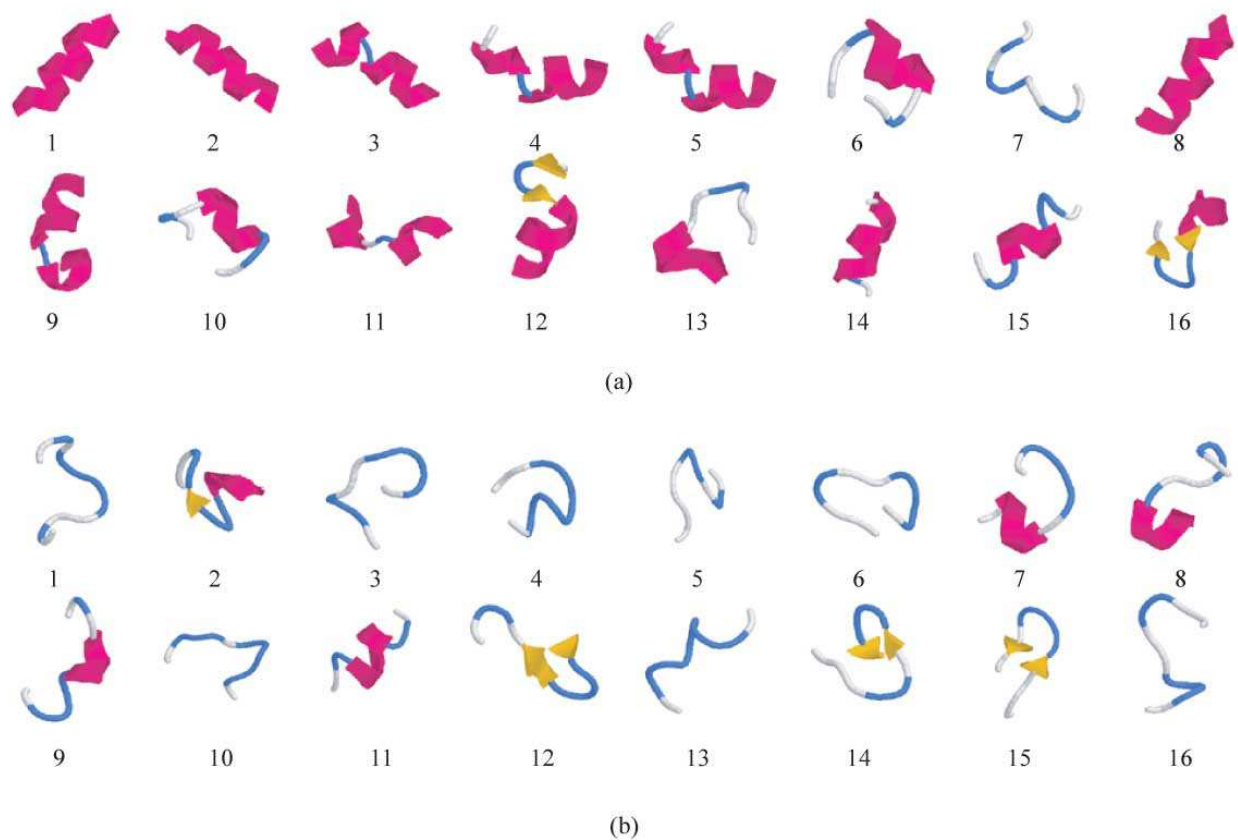


Figure 4: The lowest-energy conformations of C-peptide obtained by each of the simulated annealing MD simulations using the original AMBER parm96 (a) and the optimized force field (b). The conformations are ordered in the increasing order of energy. The figures were created with RasMol [35].

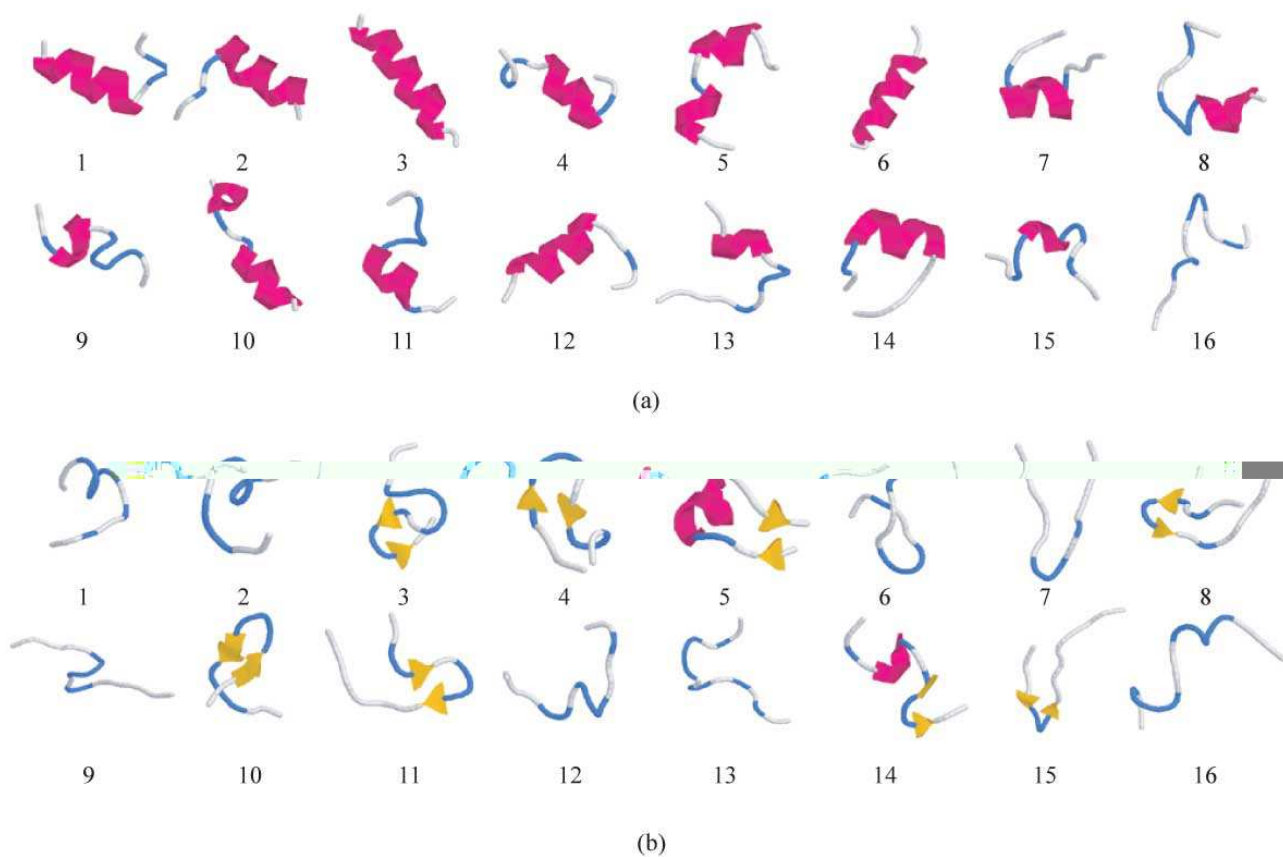


Figure 5: The lowest-energy conformations of G-peptide obtained by each of the simulated annealing MD simulations using the original AMBER parm96 (a) and the optimized force field (b). The conformations are ordered in the increasing order of energy. The figures were created with RasMol [35].